AIMS Materials Science, 9(2): 270–282.
DOI: 10.3934/matersci.2022016
Received: 12 November 2021
Revised: 13 January 2022
Accepted: 20 January 2022
Published: 02 March 2022

http://www.aimspress.com/journal/Materials

Research article

Microstructural stability of a two-phase (O + B2) alloy of the Ti–25Al–25Nb system (at.%) during thermal cycling in a hydrogen atmosphere

Nuriya Mukhamedova[1], Yernat Kozhakhmetov[1,2,*], Mazhyn Skakov[1,3], Sherzod Kurbanbekov[4] and Nurzhan Mukhamedov[1]

[1] Branch "Institute of Atomic Energy" RSE NNC RK, Kurchatov, Republic of Kazakhstan
[2] East Kazakhstan Technical University named after D. Serikbayev, Ust-Kamenogorsk, Republic of Kazakhstan
[3] National Nuclear Center of the Republic of Kazakhstan, Kurchatov, Kazakhstan
[4] H.A. Yassawi International Kazakh-Turkish University, Turkistan, Kazakhstan

* **Correspondence:** Email: kozhahmetov_e@nnc.kz; Tel: +7-775-131-68-86.

Abstract: In this work, the stability of the microstructure of the experimentally obtained two-phase (O + B2) alloy of the Ti–25Al–25Nb (at.%) system were studied during thermal cycling in a hydrogen atmosphere. It was found that the two-phase structure (O + B2) of the alloy of the Ti–Al–Nb system shows high thermodynamic stability. In this case, phase transformations of secondary phases (α2, $AlNb_2$) are observed in the microstructure of the alloy, the volumetric content of which at all stages of testing does not exceed 2%. Thus, after the first cycle of high-temperature exposure, single inclusions of the α2 phase precipitate, while in the areas enriched in Ti and Al, due to the redistribution of Nb, a new colony of the α2 phase is observed. After five test cycles, it was found that large accumulations of the α2 colony, due to the α2 → B2 phase transformations, form new micron-sized grains of the B2 phase. A volumetric accumulation of nanosized precipitates of the $AlNb_2$ phase was found near the triple joints of the grain boundaries of the B2 phase after 10 cycles of thermal exposure, which is caused by the supersaturation of B2 grains with niobium.

Keywords: Ti–Al–Nb system; thermal cycling; sorption/desorption; hydrogen; titanium aluminides; intermetallic compounds; two-phase alloy; microstructure

1. Introduction

To date, intermetallic compounds based on titanium aluminides with a high niobium content are widely studied since the role of intermetallic compounds (IMC) of the Ti–Al–Nb system as structural materials increases every year [1–8]. Along with this, these IMCs of the Ti–Al–Nb system also have a good disposition to the absorption of hydrogen and can be considered as candidate materials for solving problems of hydrogen storage [9–13]. The alloys of this system are of low density and therefore have the advantage of achieving a potentially high hydrogen storage capacity. Of all titanium aluminides, IMC based on B2, Ti_2AlNb, Ti_3Al phases [11] can contain and sorb a sufficiently large amount of hydrogen. According to the literature, in the Ti–Al system, the Ti_3Al phase can adsorb up to 4.3 wt% hydrogen [12], but its practical use is hindered by the high desorption temperature, which reaches above 800 °C. Phases based on bcc (B2, Ti_2AlNb), which arise upon the addition of Nb to Ti_3Al, can have an even greater ability to absorb hydrogen, since weakly packed structures based on bcc usually outperform close-packed structures based on fcc and hcp in hydrogen absorption. This is facilitated by the formed nanoscale phases, which have a large number of voids filled with hydrogen atoms. In addition, based on the existing knowledge about the nature of phase equilibria and transformations in the Ti–Al–Nb system [14,15], its phase state can be systematically predicted (α2(D019), β(bcc), β0(B2) and/or O). Thus, alloys of the Ti–Al–Nb system are not only candidate materials with a high ability to absorb hydrogen, but can also be used as experimental materials to study the effect of microstructure on the properties of absorption/desorption of hydrogen.

During interaction between IMS of the Ti–Al–Nb system and hydrogen, various stable and unstable hydrides are formed [16]. This is due to the phase transformations occurring in the process of sorption/desorption by hydrogen. According to literature sources, to date, IMS with a single-phase (β0(B2)) and two-phase (β(BCC)/O) structure are considered as the most promising materials for absorbing hydrogen. The structural-phase state of these alloys, namely the size and volume fraction of B2 and O-phases in the matrix, are controlled by the parameters of the initial composition consolidation method and post-experimental heat treatment. In one of the latest papers, the authors [9] found that the absorption of hydrogen by IMC in a single-phase state (β0 or B2) is limited due to phase transformations (β → ɣ) of hydrides. Apparently, the hydrogen absortion indices can be improved if the O-phase (Ti_2AlNb) is additionally introduced into the alloy [10]. In the IMC of the Ti–Al–Nb system with a single-phase structure (B2), sorption/desorption by hydrogen at low pressures leads to the formation of β-hydride, with a bcc lattice. However, in this case, β-hydride has a high stability, therefore, after its formation, dehydrogenation is impossible only if it is not heated above a temperature of 400 °C. When a single-phase IMC is heated above 400 °C, γ-hydride is additionally formed in the bulk of the material, which indicates the ongoing sorption process. The reversible transformation of hydrides β and γ occurs slowly. If the O-phase is additionally introduced into the IMS microstructure, it is possible to increase the volume of sorbed hydrogen and the rate of reverse transformation of β and γ hydrides. The formation of the orthorhombic Ti_2AlNb phase during the consolidation of the IMC of the Ti–Al–Nb system plays a key role in the accumulation of hydrogen, this is due to the fact that the two-phase O + β/B2 alloy absorbs hydrogen more actively than the single-phase β/B2 alloy due to additional interphase boundaries between O and B2/β phases.

For the full use of the IMC of the Ti–Al–Nb system as hydrogen storage devices, it is necessary to solve a number of issues and problems related to phase transformations and operational properties.

In the practical use of many metal hydrides and IMCs, difficulties arise due to the fact that absorbent materials relatively quickly lose their sorption properties with an increase in the number of hydrogen sorption/desorption cycles. During hydrogenation, monolithic samples of metal hydrides and IMCs are destroyed with the formation of fine powders, the heat flux in the layer of the absorbing material decreases, the rate of the sorption process and the achieved capacity per hydride mass unit decrease [17,18]. This is primarily due to the aggressive operating conditions of absorbent materials, which are subjected to constant cyclic exposure to high temperatures in a hydrogen atmosphere.

The technical application of metal hydrides and IMCs requires the stability of their properties during a long cycle, as well as thermal stability when exposed to high temperatures. It is clear that, depending on the content of alloyed elements, production technology and temperature conditions, it is possible in practice to obtain various hydride systems with the required structure and phase state. However, the life cycle of metal hydrides and IMCs for hydrogen storage can only be determined by simulation tests in laboratory conditions. This work is aimed at studying the microstructure of a two-phase (O + B2) alloy of the Ti–25Al–25Nb (at.%) system during thermal cycling in a hydrogen atmosphere.

2. Materials and methods

The IMCs studied in this work based on the Ti–25Al–25Nb (at.%) system were previously obtained by combining the methods of mechanoactivation (MA) and spark plasma sintering (SPS) [19,20].

Then they were subjected to heat treatment and thermocyclic processes of sorption/desorption by hydrogen. Alloy samples were quenched in water from a temperature of 900 ℃. When choosing the quenching temperature (900 ℃), the data of [21] were taken into account, where it was shown that at this temperature there is no B2 grain growth and a sufficient volume fraction of the B2 phase is fixed in the structure, capable of decomposing during subsequent aging. The choice of aging regimes for quenched alloys was based on thermal analysis data [22]. Since the recommended operating temperature according to the literature [23] does not exceed 800 ℃. Thus, it was decided to conduct aging of the alloy at 800 ℃ for 2 h. Then they were subjected to thermal cyclic processes of sorption/desorption by hydrogen. The parameters of thermal cycling experiments are presented in Table 1.

Table 1. Parameters for thermal cycling experiments.

Absorption temperature (℃)	Desorption temperature (℃)	Sampling	Exposure at each stage (min)
500	500	1 cycle	120
		5 cycle	
		10 cycle	

Cyclic experiments on sorption/desorption with alloy samples of the Ti–25Al–25Nb (at.%) system were carried out in the VIKA experimental unit [24]. The VIKA unit is intended for research with irradiated and non-irradiated samples of materials from nuclear and fusion reactors by thermal desorption method in the temperature range from 20 to 1500 ℃. Figure 1 shows a general view of

the unit and the working chamber.

The microstructure and elemental composition of the obtained IMCs were investigated in topographic and compositional contrast mode using a TescanVega3 scanning electron microscope with an Oxford X-Act energy dispersive spectral analysis attachment. Measuring of the geometric dimensions of the identified phases, as well as determining their area and volume fraction (selecting objects with a close gray level in the image and measuring the area occupied by these objects) was conducted using the Essence™ software module of the TescanVega3 scanning electron microscope.

X-ray structural studies were conducted on an EMPYREAN diffractometer with a Rentgen-Master control computer system. X-ray diffraction patterns were obtained using monochromatic CuK α-radiation at an accelerating voltage of 45 kV and an anode current of 40 mA with a 2θ scanning interval: 10°–135° and a pitch of 0.026°. Radiographs were decoded using the Crystallography Open Database (COD).

The fine structure of the obtained materials after heat treatment was investigated using a transmission electron microscope (TEM) FEI Tecnai 20 G2 TWIN, with a maximum accelerating voltage of 200 kV. Decoding of electron diffraction patterns and preparation of samples were conducted according to the standard technique described in the paper [25].

(a)

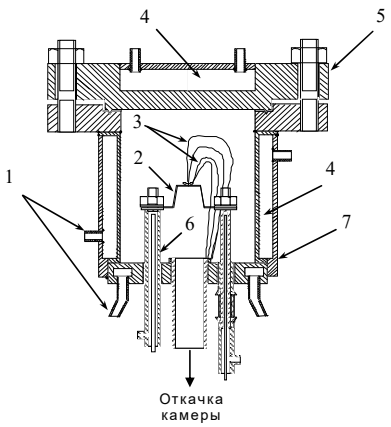

(b)

Figure 1. VIKA Experimental Unit [24]. (a) General view; (b) TDS-chamber: 1—water-cooling branch pipes; 2—tantalum heater with crucible; 3—WR thermocouples; 4—water-cooling circuit; 5—lid-flange of vacuum chamber; 6—current leads; 7—vacuum chamber vessel.

3. Results and discussion

Figure 2 shows SEM images of the microstructure of the Ti–Al–Nb system alloy before thermal cycling. As shown in the figure, the alloy has a completely lamellar two-phase microstructure, which for these alloys was achieved by two-stage heat treatment in an inert atmosphere. The microstructure consists of grains of the B2 phase (gray matrix) which are outlined along the perimeter by precipitated plates of the O phase (dark gray), at the same time in the body of the B2 phase grains there are lamellar colonies of the O phase with interlocked and thin boundaries. The microstructure

contains only a small amount of globular and lineal precipitates of the α2 phase.

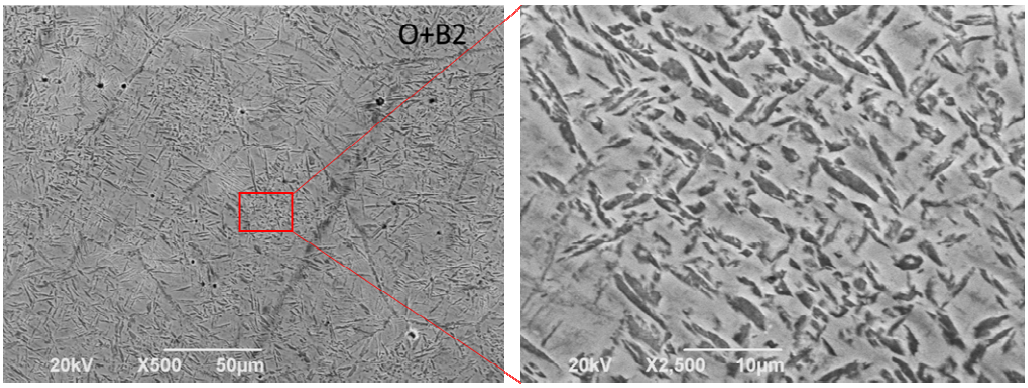

Figure 2. Two-phase (B2 + O) microstructure of alloys of the Ti–Al–Nb system after high-temperature treatment.

Figure 3 shows typical TEM images of the O and α2 phase precipitates at the grain boundaries of the B2 phase. The red circles in the microphotographs indicate the areas from which the diffraction was taken. Dark contrasting particles (Figure 3a) represent the line highlighting of the α2 phase. Particles of the α2 phase are observed both at the boundaries of the O phase colonies and at the grain boundaries of the B2 phase. However, there is no crystallographic orientation relationship between the α2 and B2 phases, as well as the α2 and O phases. In this case, some colonies of line particles of the α2 phase tend to precipitate at the triple grain boundaries of the B2 phase; most likely, the nucleation of particles of the α2 phase at the triple grain boundaries of the B2 phase is due to the energy advantage.

According to the results, the sizes and shapes (Figure 3b) of the O phase in the initial samples depend on the distribution and vary over a wide range of values from 100 nm to 6 μm. The elemental composition of the matrix grains B2 and the precipitated particles of the O, α2 phases in the alloys are shown in Table 2. It was found that the B2 phase is slightly enriched in Nb, but depleted in Al compared to precipitates of the O phase at the grain boundaries. At the same time, Table shows, the content of Ti in the α2 phase is an order of magnitude higher than in the B2 phase (20–24 at.%). The elemental composition of the B2 and O phases is close to each other, which complicates identifying of the phases (Table 2). As can be seen from Figure 3b, visual contrast of the B2 phase can differ from grain to grain, and this is primarily due to the difference in the content of Ti and Al within 2–4 (at.%). It is assumed that the diffusion of dissolved atoms is more sensitive to temperature, and the composition of the B2 phase can be different depending on the temperature, rate and duration of heating-cooling. The Nb content in the grains of the B2 phase varies within a value of 1–3 (at.%).

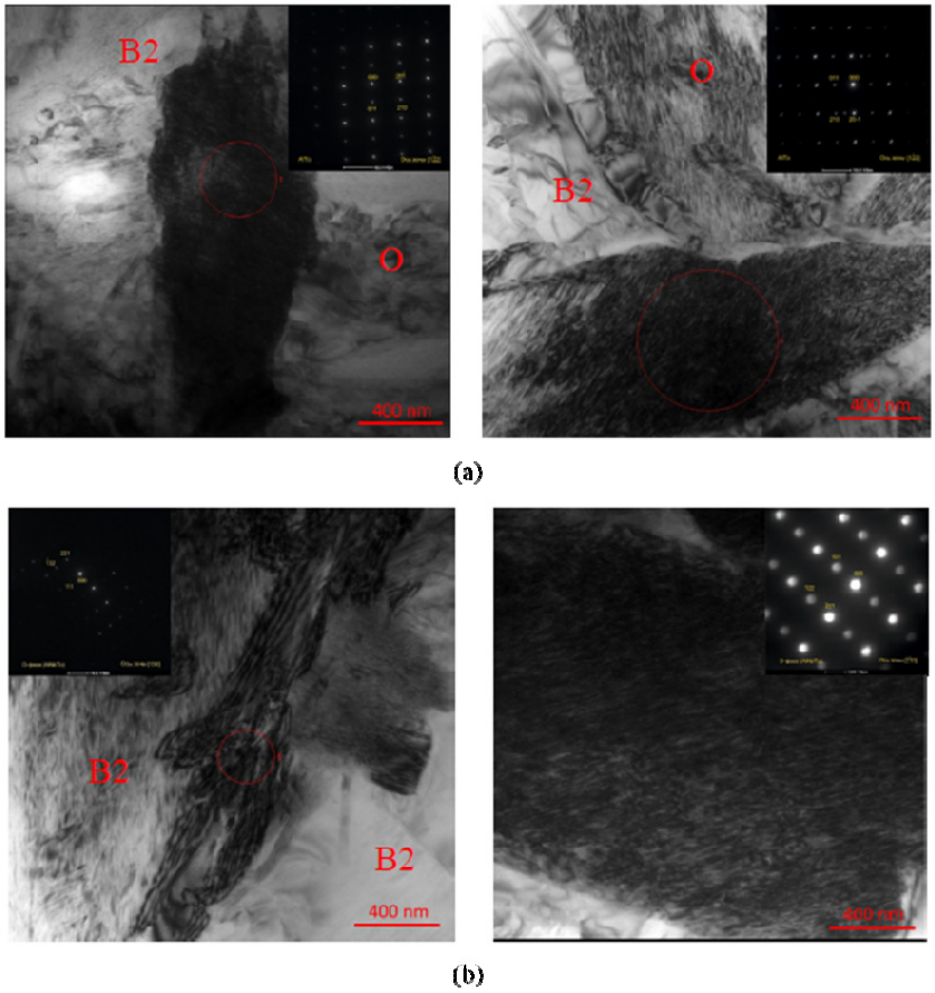

Figure 3. Bright-field TEM microphotography of Ti_2AlNb and Ti_3Al phases in the B2 phase matrix. (a) Ti_3Al (α2), (b) Ti_2AlNb (O).

Table 2. Results of local elemental analysis (wt%).

Ti	Al	Nb	Фаза
69.30	23.48	7.22	α2
72.12	21.16	6.72	α2
48.18	22.18	29.64	B2
48.32	23.87	27.81	B2
53.23	25.99	20.78	O
51.58	26.48	21.93	O

After one cycle of thermal action in a hydrogen atmosphere, the distribution of the main phases almost did not undergo any visible changes. As can be seen from Figure 4, after one cycle of thermal loading at a temperature of 500 °C, precipitation of globular precipitates of the α2 phase (Figure 4) is observed both at the boundaries and in the body of B2 grains.

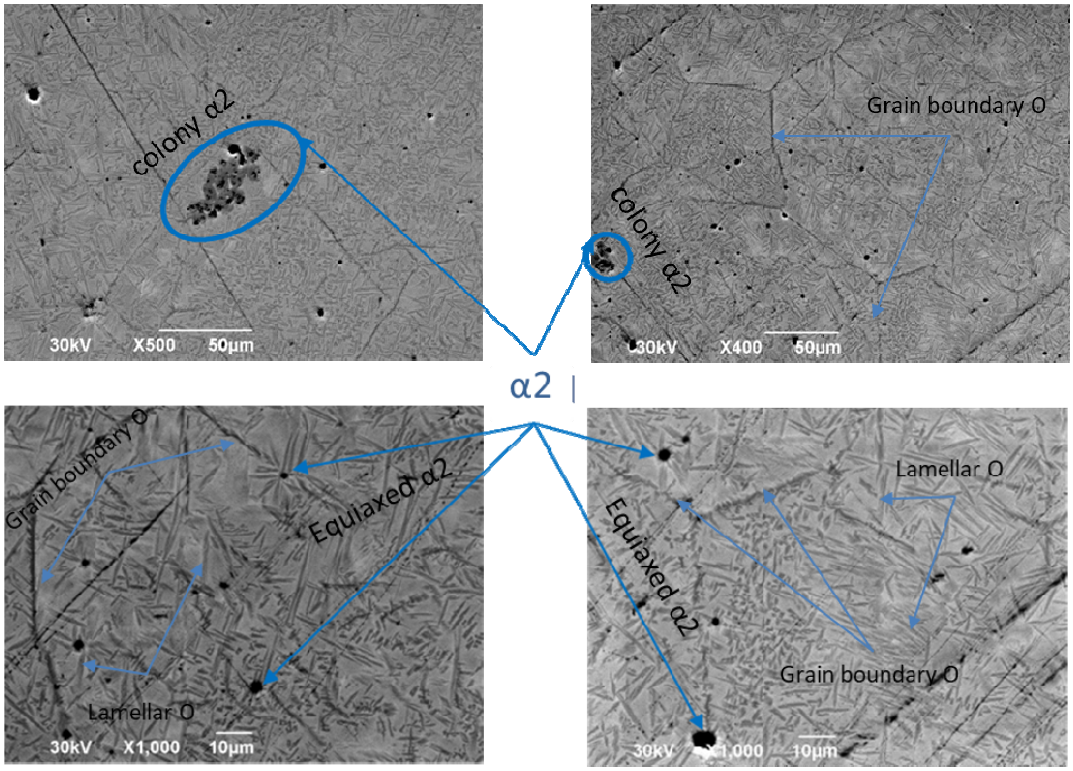

Figure 4. SEM image of the Ti–Al–Nb alloy microstructure after one sorption/desorption cycle (Main matrix, light gray-phase B2).

In this case, in the grain body of the B2 phase (Figure 5), in separate local areas, an accumulation of a colony of the α2 phase of a predominantly spherical shape is observed, most likely due to the redistribution of Nb between the main phases (O and B2). It should be added that after one cycle of thermal treatment in a hydrogen medium at the boundaries and in the body of grains of the B2 phase, an increase in the amount of precipitates of α2, a globular type phase, is observed. According to the results, after the first cycle of thermal exposure in a hydrogen atmosphere, due to phase transformations in the grains of the B2 phase with a predominance of Ti and Nb, coarser and larger accumulations of the α2 phase colony (50–100 μm) are formed, while in grains with a predominance of Al, the formation of smaller α2 colonies (10–50 μm) was observed.

The subsequent increase in the amount of thermal cycling loading in a hydrogen atmosphere almost does not lead to visible changes in the test sample microstructure (Figure 6). For some difference, the complete absence of precipitate accumulations of phases α2 colonies can be taken. A similar situation persists after 10 cycles of hydrogen saturation. No changes in the sizes of the B2 and O phases are observed either after 5 cycles or after 10 cycles. The stability in the structure of the main phases (B2 + O) under multiple high-temperature cyclic influences in a hydrogen atmosphere can be a consequence of low values of the diffusion coefficients of Ti and Nb.

At the same time, in the structure of the test samples after thermal cycling at a temperature of 500 °C, the formation of B2 phase grains was found, which were tens times smaller in size compared to the sizes of the original B2 grains. The formed B2 grains, according to the authors of [26], were transformed from the α2 phase colony. Since the separation coefficient (distribution coefficient, k) of the elements of the phase components α2 and B2 is close to one, due to this fact, the

metastable phase α2 transforms into B2 grains. The converted B2 grains will gradually increase in size under the influence of thermal action, and then will merge into the B2 matrix. A similar situation is especially typical for areas with an accumulation of large colonies of the α2 phase, which is explained by the need to achieve an optimal balance due to a decrease in the content of the metastable phase α2.

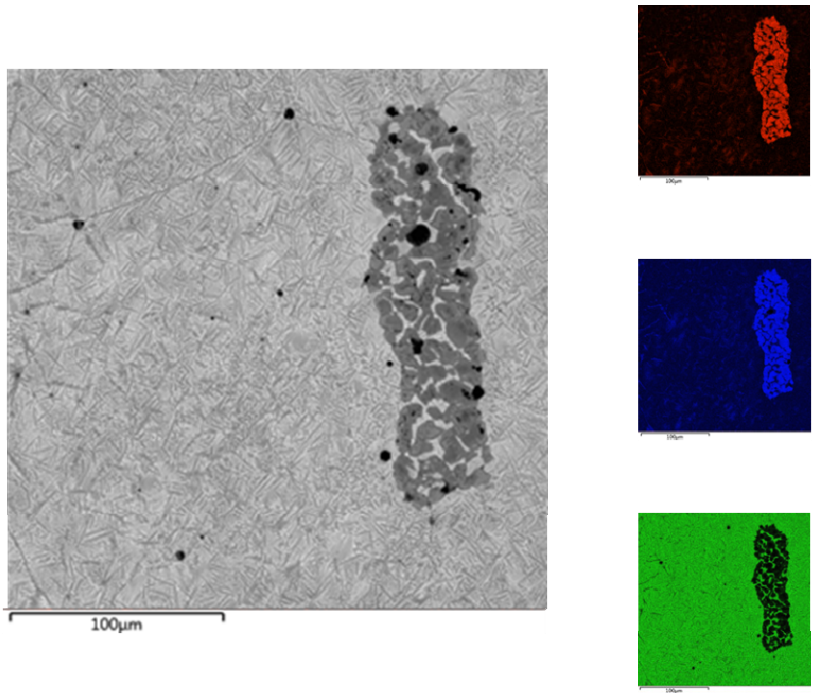

Figure 5. Microstructure mapping of Ti–Al–Nb system alloys after one sorption/desorption cycle (red Ti, blue Al, green Nb).

A volumetric accumulation of nanosized precipitates is observed near the triple joints of the grain boundaries of the B2 phase, after 10 cycles of thermal action (see Figure 6, shown by red arrows). It is not possible to determine the elemental composition of these materials using SEM and EDS because of their small size. However, according to the results of elemental analysis of large areas with accumulation areas of these precipitates, an increased content of Nb and Al is observed, which allows identifying these precipitates as the $AlNb_2$ phase with a certain degree of caution. The precipitation of precipitates of the $AlNb_2$ phase can be caused by the supersaturation of Nb; a more detailed mechanism of phase transformations and decomposition in TiAl alloys with a high Nb content was considered in [27]. However, at present the internal mechanism of the $AlNb_2$-phase precipitation in the region of triple joints of B2 grains after thermal cycling is not clear. Both the O phase and the B2 phase grains in the region of triple joints can be responsible for the precipitation of the $AlNb_2$ phase. Moreover, $AlNb_2$ precipitated in the region of B2 and O phases should have certain orientational relations with the matrix B2. This research identified only the precipitated phases in the region of triple junctions of B2 grains. The mechanism of the appearance of the $AlNb_2$-phase in the region of triple junctions of B2 grains requires a more detailed study.

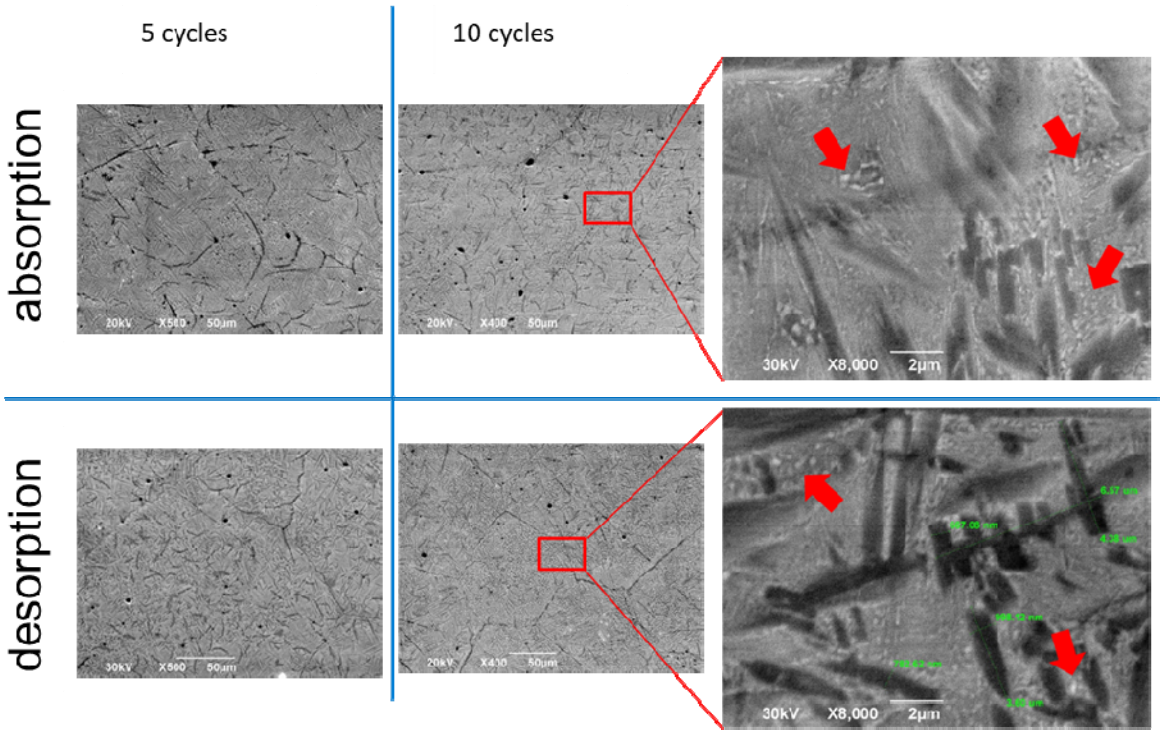

Figure 6. SEM image of the Ti–Al–Nb alloy microstructure after 5 and 10 sorption/desorption cycles.

Figure 7 shows the increased intensity fragments of the diffraction patterns of the samples after thermal cycling loading in a hydrogen atmosphere. Due to the fact that the conditions for recording the diffraction patterns of the sample before and after saturation with hydrogen were identical, changes in the detailing of the peaks identified by the O-phase lines most likely most realistically and accurately reflect the actual changes in the state of the phase structure.

The angular positions of the lines of bar diagrams are calculated for possible variants of the phase composition with the selection of the corresponding values of the lattice parameters. The line intensities on the bar charts correspond to the intensities of the lines of the tabular phases. Changes in the phase composition are manifested by the appearance of a diffraction peak with a diffraction angle of about 40.6 °2θ. This peak is located near the peak corresponding to the line (221) of the O-phase with an orthorhombic lattice, the lines of which are quite confidently identified with the peaks in the diffraction pattern of the initial sample. The presence and increase in the intensity of this peak is the most obvious and characteristic change in the diffraction pattern from the surfaces of the samples in the series: ref.-1 cycle-5 cycles-10 cycles.

The selection of the candidate phase, the lines of which have a satisfactory correspondence to the additional peak, leads to a good coincidence of the diffraction peaks in the diffraction patterns of the B2 type phase, which was previously identified in the phase composition of the initial sample. Most of the intense lines of this phase have close coincidences in angular positions also with the lines of O *-$AlNbTi_2$ (CmCm; a = 5.9 Å; b = 9.60 Å; c = 4.67 Å) of the orthorhombic phase, the lattice parameters of which differ from the initial ones. The formation of an orthorhombic phase with altered lattice parameters will probably be more preferable when interpreting the results of structural changes after experiments on hydrogen saturation. It should be noted that the alloy underwent the

greatest structural transformation after cycle 10 of thermal cycling.

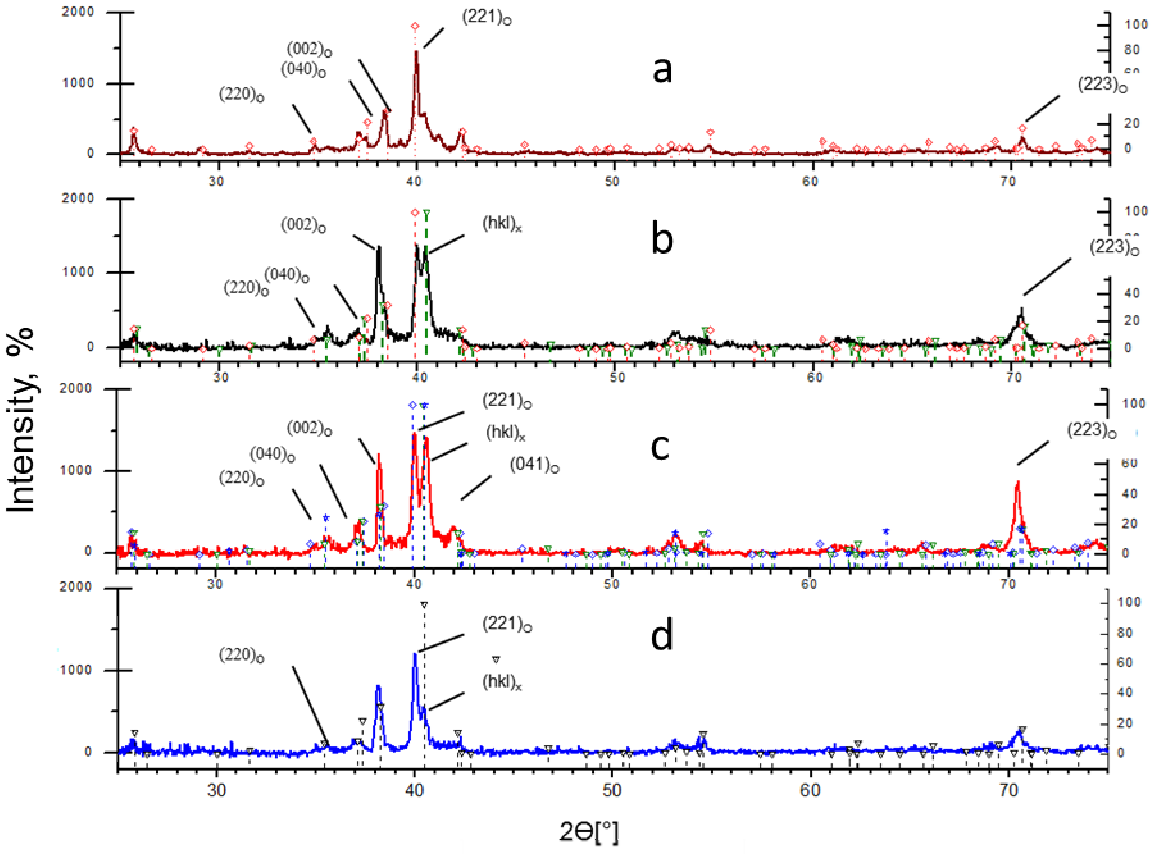

Figure 7. XRD results for the Ti–25Al–25Nb (at.%) composition material: (a) initial sample, (b) after 1 cycle, (c) after 5 cycles, (d) after 10 cycles.

In addition, on the sample after 10 cycles, a number of peaks coincide well with the positions of the lines of the Nb_2Al type phase (P42/mnm; a = 9.94 Å, c = 5.186 Å), this indirectly confirms the identification of the previously detected precipitates. Illustrations of changes in the diffraction patterns of alloys as a result of thermal exposure to hydrogen in an atmosphere of hydrogen are shown in Figures 7d.

Changes in the diffraction pattern of the sample as a result of successively performed saturation and desorption are most clearly manifested in the change in the relative and absolute intensities of the peaks in the range of 39–41°2θ angles. The intensity of the peak with an angular position of 40.6°2θ after saturation increases to the intensity level of the peak with an angular position of 40.0° and exceeds its intensity after desorption.

The lines of such phases as, for example, B2 (3.317 Å) and o-$AlNbTi_2$ (CmCm; a = 6.09 Å; b = 9.85 Å; c = 4.68 Å), their lattice parameters differ from the tabular ones.

The observed changes may well be described as structural transformations in which the predominantly two-phase structure of the alloys, fixed in the initial state, undergoes a transformation with the formation of a new structure. The results of X-ray diffraction studies of the samples do not reveal the formation of hydrides in the form of independent phases that have their own type of crystal lattice, which is different from the previously detected phases. The absorption of hydrogen at

saturation can most likely be associated with the formation of an ordered or disordered solid solution of interstitial on the basis of already existing crystalline phases. According to the results of the alloy sample analysis, the transformation mechanism of the phase composition at saturation, apparently, should be considered as a shift due to the simultaneous presence of phases of the original and modified compositions in the diffraction patterns. In the case of determining the transformed phase as an interstitial solution in the O-$AlNbTi_2$ phase, the presence of separating peaks corresponding to two compositions of solutions without a smooth transition speaks in favor of this assumption. At the same time, according to the results of the analysis of alloy samples, the transformation mechanism of the phase composition at saturation, on the contrary, can be defined as diffuse, occurring with a gradual change in the lattice parameters as hydrogen is absorbed, which follows from a clear separation of the peaks of the initial and transformed phases.

4. Conclusions

(1) Thus, according to the results of implemented works on studies of microstructure of the two-phase (O + B2) alloy of the Ti–25Al–25Nb (at.%) system In the process of thermal cycling in a hydrogen atmosphere, the following conclusions can be drawn:
(2) After one cycle of thermal action in a hydrogen atmosphere, the Ti–25Al–25Nb (at.%) alloy retains its two-phase microstructure. The precipitation of single precipitates of the α2 phase is observed in the entire volume of the material. In local areas, an accumulation of a phase α2 colony of a predominantly spherical shape is observed, most likely due to the redistribution of Nb between the main phases (O and B2).
(3) Grains B2 with a size of less than 10 microns are formed in areas with an accumulation of large colonies of spherical α2-phases, as a result of α2 → B2 phase transformation. During thermal exposure, metastable precipitates of the α2-phase tend to achieve structural balance in the alloy, decomposing into the B2 phase. In addition, defects in the B2 + O interfaces and microsegregation of alloy elements at the interface also contribute to the nucleation of B2 grains.
(4) An increase in the amount of thermal cycling loading in a hydrogen atmosphere almost does not lead to visible changes in the morphology of the main phases. At the same time, near the triple joints of grain boundaries of the B2 phase, after 10 cycles of thermal exposure, a volumetric accumulation of newly formed nanosized precipitates of the AlNb2 phase is observed, which is most likely caused by the supersaturation of B2 grains with niobium.
(5) Under multiple thermal cycling in a hydrogen atmosphere, the predominantly two-phase structure of the alloys undergoes transformation with the formation of a new structure. In the phase composition of the samples, the formation of hydrides in the form of independent phases was not revealed. The absorption of hydrogen can most likely be associated with the formation of an ordered or disordered solid solution of interstitiality based on already existing crystalline phases.

Acknowledgments

This research has is funded by the Science Committee of the Ministry of Education and Science of the Republic of Kazakhstan (Grant No. BR10965284)

Conflict of interest

All authors declare no conflicts of interest in this paper.

References

1. Banerjee D, Gogia AK, Nandy TK, et al. (1988) A new ordered orthorombic phase in a Ti_3Al–Nb alloy. *Acta Metall* 36: 871–882. https://doi.org/10.1016/0001-6160(88)90141-1
2. Singh N, Acharya S, Prashanth KG, et al. (2021) Ti6Al7Nb-based TiB-reinforced composites by selective laser melting. *J Mater Res* 36: 3691–3700. https://doi.org/10.1557/s43578-021-00238-x
3. Hagiwara M, Kitashima T, Emura S, et al. (2019) Very high-cycle fatigue and high-cycle fatigue of minor boron-modified Ti–6Al–4V alloy. *Mater Trans* 60: 2213–2222. https://doi.org/10.2320/matertrans.MT-M2019169
4. Liu B, Liu Y, Qiu C, et al. (2015) Design of low-cost titanium aluminide intermetallics. *J Alloy Compd* 640: 298–304. https://doi.org/10.1016/j.jallcom.2015.03.239
5. Dong S, Chen R, Guo J, et al. (2015) Effect of power on microstructure and mechanical properties of $Ti_{44}Al_6Nb_{1.0}Cr_{2.0}V_{0.15}Y_{0.1}B$ alloy prepared by cold crucible directional solidification. *Mater Design* 67: 390–397. https://doi.org/10.1016/j.matdes.2014.12.006
6. Popela T, Vojtěch D, Vogt JB, et al. (2014) Structural, mechanical and oxidation characteristics of siliconized Ti–Al-X (X = Nb, Ta) alloys. *Appl Surf Sci* 307: 579–588. https://doi.org/10.1016/j.apsusc.2014.04.076
7. Chen R, Fang H, Chai D, et al. (2017) A novel method to directional solidification of TiAlNb alloys by mixing binary TiAl ingot and Nb wire. *Mater Sci Eng A-Struct* 687: 181–192. https://doi.org/10.1016/j.msea.2017.01.078
8. Kenel C, Leinenbach C (2016) Influence of Nb and Mo on microstructure formation of rapidly solidified ternary Ti–Al–(Nb, Mo) alloys. *Intermetallics* 69: 82–89. https://doi.org/10.1016/j.intermet.2015.10.018
9. Zhang LT, Ito K, Vasudevan VK, et al. (2001) Hydrogen absorption and desorption in a B2 single-phase Ti–22Al–27Nb alloy before and after deformation. *Acta Mater* 49: 751–758. https://doi.org/10.1016/S1359-6454(00)00400-6
10. Umarova OZ, Pogozha VA, Buranshina RR (2017) Formation of structure and mechanical properties of heat-resistant alloy based on titanium aluminide during heat treatment. *Bull Moscow Aviation Institute* 24: 160–169 (in Russian).
11. Ito K, Zhang LT, Vasudevan VK, et al. (2001) Multiphase and microstructure effects on the hydrogen absorption/desorption behavior of a Ti–22Al–27Nb alloy. *Acta Mater* 49: 963–972. https://doi.org/10.1016/S1359-6454(00)00402-X
12. Kazantseva NV, Mushnikov NV, Popov AA, et al. (2008) Nanosized hydrides of titanium aluminides. *Phys Technol High Press* 18: 147–151 (in Russian).
13. Karakozov BK (2018) Study of absorption-desorption of hydrogen with an alloy based on the Ti–Al–Nb system. *Polzunovsky Bull* 2: 154–159 (in Russian).
14. Belmonte N, Girgenti V, Florian P, et al. (2016) A comparison of energy storage from renewable sources through batteries and fuel cells: A case study in Turin, Italy. *Int J Hydrogen Energ* 41: 21427–21438. https://doi.org/10.1016/j.ijhydene.2016.07.260

15. Friedrichs O, Klassen T, Sánchez-López JC, et al. (2006) Hydrogen sorption improvement of nanocrystalline MgH_2 by Nb_2O_5 nanoparticles. *Scripta Mater* 54: 1293–1297. https://doi.org/10.1016/j.scriptamat.2005.12.011
16. Raghavan V (2010) Al–Nb–Ti (Aluminum–Niobium–Titanium). *JPEDAV* 31: 47–52. https://doi.org/10.1007/s11669-009-9623-x
17. Sakintuna B, Lamari-Darkrim F, Hirscher M (2007) Metal hydride materials for solid hydrogen storage: a review. *Int J Hydrogen Energ* 32: 1121–1140. https://doi.org/10.1016/j.ijhydene.2006.11.022
18. Gambini M, Stilo T, Vellini M, et al. (2017) High temperature metal hydrides for energy systems Part A: numerical model validation and calibration. *Int J Hydrogen Energ* 42: 16195–16202. https://doi.org/10.1016/j.ijhydene.2017.05.062
19. Kozhakhmetov Ye, Skakov M, Mukhamedova N, et al. (2021) Changes in the microstructural state of Ti–Al–Nb-based alloys depending on the temperature cycle during spark plasma sintering. *Mater Test* 63: 119–123. https://doi.org/10.1515/mt-2020-0017
20. Kozhakhmetov YA, Skakov MK, Kurbanbekov SR, et al. (2021) Powder composition structurization of the Ti–25Al–25Nb (at.%) system upon mechanical activation and subsequent spark plasma sintering. *Eurasian Chem-Techno* 23: 37–44. https://doi.org/10.18321/ectj1032
21. Popov AA, Illarionov AG, Grib SV, et al. (2008) Phase and structural transformations in an alloy based on orthorhombic titanium aluminide. *Phys Metal Metal Sci* 106: 414–425 (in Russian). https://doi.org/10.1134/S0031918X08100104
22. Khadzhieva OG, Illarionov AG, Popov AA, et al. (2013) Effect of hydrogen on the structure of a hardened alloy based on orthorhombic titanium aluminide and phase transformations during subsequent heating. *Phys Metal Metal Sci* 114: 577–582 (in Russian). https://doi.org/10.1134/S0031918X13060070
23. Polkin IS, Kolachev BA, Ilyin AA (1997) Titanium aluminides and alloys based on them. *Technol Light Alloy* 3: 32–39(in Russian).
24. Kurbanbekov ShR, Aydarova MT, Stepanova OA, et al. (2018) Determination of the sorption properties of a material based on the Ti–Al–Nb system. *Bull Shakarim State University of the city of Semey* 3: 68–72 (in Russian).
25. Utevsky L (1973) Diffraction electron microscopy in metallurgy, Moscow: Metallurgy, 584 (in Russian).
26. Chen Z, Cai Z, Jiang X, et al. (2020) Microstructure evolution of Ti–45Al–8.5Nb–0.2W–0.2B–0.02Y alloy during long-term thermal exposure. *Materials* 13: 1–14. https://doi.org/10.3390/ma13071638
27. Song L, Xu XJ, You L, et al. (2014) Phase transformation and decomposition mechanisms of the βo(ω) phase in cast high Nb containing TiAl alloy. *J Alloy Compd* 616: 483–491. https://doi.org/10.1016/j.jallcom.2014.07.130

AIMS Press